ACS APPLIED MATERIALS & INTERFACES

Research Article

www.acsami.org

Enhanced Visible Light-Induced Charge Separation and Charge Transport in Cu_2O-Based Photocathodes by Urea Treatment

Peng Wang,[†] Yiming Tang,[†] Xiaoming Wen,[‡] Rose Amal,*[,†] and Yun Hau Ng*[,†]

[†]Particles and Catalysis Research Group, School of Chemical Engineering, The University of New South Wales, Sydney, NSW 2052, Australia

[‡]School of Photovoltaics and Renewable Energy Engineering, The University of New South Wales, Sydney, NSW 2052, Australia

Supporting Information

ABSTRACT: Carrier density, photocharge transfer kinetics, and charge transfer resistance of the anodized Cu−Cu_2O−CuO photocathode were greatly improved using thermal treatment with urea. Time-correlated single-photon counting (TCSPC) results revealed the faster electron transfer kinetics from Cu_2O to CuO in the urea-treated Cu−Cu_2O−CuO composite photoelectrodes. Preservation of the metallic copper component via the intermediate Cu_3N during the treatment facilitated higher bulk conductance of the Cu−Cu_2O−CuO photocathode for improved charge transport. Higher carrier density was also observed in the urea-treated photoelectrode, which was possibly attributed to the presence of nitrogen as a dopant. Furthermore, the compact outer layer of CuO protected the underlayer Cu_2O from being in direct contact with the aqueous solution. This suppressed the photocorrosion of Cu_2O and resulted in the higher photostability of the Cu−Cu_2O−CuO film. When these advantages were combined, the urea-treated Cu−Cu_2O−CuO film showed a higher photocurrent of 2.2 mA/cm^2 and improved stability versus that of the conventional Cu−Cu_2O−CuO film (1.2 mA/cm^2). To improve the charge transfer kinetics and carrier density, this paper provides a new strategy for synthesizing effective and stable Cu_2O-based photoelectrodes by using urea treatment.

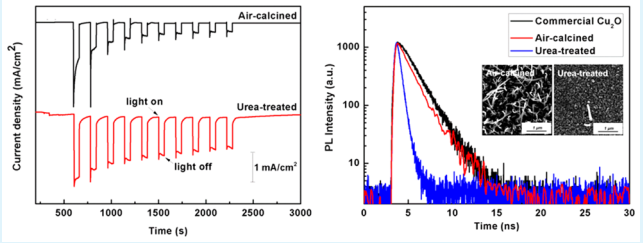

KEYWORDS: *Cu_2O photocathode, photoelectrochemical cells, electron transport, electron lifetime, urea treatment*

1. INTRODUCTION

Because of its abundance and nontoxic nature, cuprous oxide (Cu_2O) has shown great potential in light-driven applications, including solar generation of hydrogen from water, photochemical sensors, and photovoltaic devices.[1−4] It is normally found as an intrinsic p-type semiconductor with a direct bandgap of 2.0−2.2 eV. With its relatively high absorption coefficient of up to ~10^4 cm^{-1} and a high theoretical photocurrent density of 14.7 mA/cm^2 under light intensity of 1 sun, it has been regarded as a promising candidate for the solar conversion applications.[5,6] Even though the theoretical energy conversion efficiency for a Cu_2O-based thin film solar cell is ~20% according to Shockley−Queisser calculations,[7] the highest reported energy conversion efficiency was <4%.[3] The low efficiency is believed to be associated with the imperfect crystal structure that resulted from the atomic vacancies created by either excessive copper or deficient oxygen. The type and amount of vacancies determine the p- or n-type conducting behavior of Cu_2O. These atomic vacancies affect the overall carrier density and charge transport in Cu_2O. It is widely accepted that doping is a common and effective strategy for controlling the atomic vacancies in a semiconductor and subsequently influence its charge transport in a photoelectrochemical environment.[8−11] To replenish the vacancies created by oxygen (copper excess or oxygen deficient) for better p-type conducting properties, nitrogen treatments of Cu_2O-based electrodes using various methods have been reported.[12−14] There are a number of studies of the effects of nitrogen treatment on the structural, optical, and electrical properties of Cu_2O films.[15−17] To the best of our knowledge, most of the attempts to incorporate nitrogen into Cu_2O-based films relied on the use of a reactive radiofrequency (rf) magnetron sputtering method using nitrogen as the reactive gas. It has been demonstrated that the bandgap and resistivity of Cu_2O could be tuned by controlling the gas flow of nitrogen and deposition pressure.[18] Ishizuka's group reported a 2 order of magnitude increase in carrier density, and a low resistivity of 15.2 Ω m when Cu_2O was doped with nitrogen.[14] Malerba's work showed a decrease in resistivity from 86.5 Ω cm for the intrinsic Cu_2O to 1.14 Ω cm upon nitrogen treatment.[13] Siah et al. reported that the hole concentration of the Cu_2O film increased from 3.7 × 10^{15} to 1.8 × 10^{18} cm^{-3} after the introduction of nitrogen.[19]

Ammonia has also been reported as a nitrogen source for the treatment of TiO_2 to extend its light absorption into visible light range (λ < 500 nm).[20] However, the use of ammonia may lead to safety and environmental issues because of its toxic and flammable properties. In this work, we report for the first time

Received: March 19, 2015
Accepted: August 25, 2015
Published: August 25, 2015

DOI: 10.1021/acsami.5b06601
ACS Appl. Mater. Interfaces 2015, 7, 19887−19893

the use of urea as the nitrogen source to treat the anodized Cu_2O-based thin film. Urea is considered as a safer and more environmentally friendly nitrogen source, compared to ammonia. The urea-treated anodized Cu foil consists of a mixture of Cu−Cu_2O−CuO, with a high proportion of Cu metal being preserved. The thin film exhibited a significant enhancement of charge carrier density. Because of the presence of the conducting pathway (metallic Cu) and the likelihood of nitrogen doping, a lower charge transfer resistance of the urea-treated Cu−Cu_2O−CuO thin film was observed. From the photoelectrochemical measurement, the urea-treated Cu−Cu_2O−CuO thin film showed a higher photocurrent of 2.20 mA/cm^2, compared with the photocurrent of 1.20 mA/cm^2 of the conventionally air-calcined Cu−Cu_2O−CuO thin film. As opposed to the commonly used reactive radiofrequency magnetron sputtering, this work provides a promising alternative in treating Cu_2O-based photoeletrodes with a nitrogen source.

2. EXPERIMENTAL SECTION

2.1. Preparation of Urea-Treated Cu−Cu_2O−CuO Photoelectrodes. The as-anodized Cu_2O thin film was synthesized by anodization of pure Cu foil (99.9%, Aldrich) in an ethylene glycol (>99%, Aldrich)-based alkaline electrolyte at 10 V for 10 min.[21] The voltage was supplied by a programmable dc power supply (PST-3201, GW Instek). Using a home-designed two-electrode anodization cell, Cu foil was applied as a working electrode, and Pt foil was used as a counter electrode. The anodization electrolyte consisted of 0.75 wt % potassium hydroxide (>99%, Aldrich), 3.0 wt % Milli-Q water, and 0.20 wt % sodium fluoride (>99%, Aldrich), the rest being ethylene glycol. The air-calcined Cu−Cu_2O−CuO thin film was then prepared by calcination of the as-anodized Cu_2O thin film at 400 °C for 1 h in an air atmosphere (with a ramping rate of 5 °C/min). For the urea-treated Cu−Cu_2O−CuO thin film, the as-anodized Cu_2O thin film was first calcined with 100 mg of urea at 400 °C for 3 h in a N_2 atmosphere, followed by the second calcination at 400 °C for 1 h in an air atmosphere with the same ramping rate. The anodized Cu_2O thin film and 100 mg of urea were placed separately in a porcelain boat with urea at the upstream side of the furnace. Before the anodized thin film had been thermally treated with urea, the tube furnace was purged with N_2 gas for 1 h to remove air inside it. The whole urea treatment process was conducted under a N_2 atmosphere with a N_2 flow rate of 25.0 mL/min. To understand the effect of annealing with urea in a N_2 atmosphere on the transformation of the as-anodized Cu_2O film to the copper composite photoelectrode, the as-anodized Cu_2O thin film after treatment with 100 mg of urea at 400 °C for 3 h in a N_2 atmosphere was prepared and studied (see Figures S1 and S2 of the Supporting Information).

2.2. Characterization of Urea-Treated Cu−Cu_2O−CuO Photoelectrodes. The morphology of the air-calcined and urea-treated Cu−Cu_2O−CuO thin film was studied using scanning electron microscopy (SEM) (S900, Hitachi). The thickness of the copper oxide layer was measured by a field emission scanning electron microscope (NanoSEM 230, FEI Nova). The cystallinity and composition were examined by an X-ray diffractometer (PANalytical Empyrean). The existence of nitrogen was detected by an X-ray photoemission spectrometer (ESCALAB220i-XL, Thermo Scientific) with Al Kα radiation at 1486.6 eV. All the X-ray photoemission spectrometry (XPS) data were calibrated by the carbon 1s peak at 285 eV. The conduction type and carrier concentration were investigated using Mott−Schottky (MS) measurements at a frequency of 10 kHz in the dark (PG STAT-302N, Autolab). The charge transfer resistance was measured by electrochemical impedance spectroscopy (EIS) measurements at a voltage of 0.25 V versus RHE in dark. The UV−vis diffuse reflectance property was measured by a UV/vis/NIR spectrophotometer (PerkinElmer LAMBDA 1050) with GaP (1200−900 nm) and Si (900−250 nm) detectors. The fluorescence lifetime was measured using a time-correlated single-photon counting (TCSPC) technique on a Microtime-200 system (Picoquant) with excitation via a 405 nm laser. The photoelectrochemical responses were recorded by chronoamperometry measurements in a standard three-electrode photoelectrochemical cell under on−off illumination cycles using a 300 W xenon lamp with a cutoff filter (λ = 420 nm). The photoelectrochemical cell was made of a Cu−Cu_2O−CuO thin film working electrode, a Ag/AgCl reference electrode, and a Pt counter electrode. The applied voltage was fixed at 0.25 V versus RHE (−0.36 V vs Ag/AgCl). A 0.5 M K_2SO_4 solution was utilized as the electrolyte for all electrochemical measurements.

3. RESULTS AND DISCUSSION

SEM top-view images shown in panels a and b of Figure 1 illustrate the surface morphological differences of the air-calcined and urea-treated Cu−Cu_2O−CuO composite photoelectrodes. On the basis of high-resolution transmission electron microscopy analysis in our earlier work, the air-calcined thin film was composed of an underlayer of Cu_2O embedded with a dense layer of nanowires.[21,22] These nanowires on the surface of the film were identified as CuO. In contrast, the urea-treated thin film showed a considerably flat surface with compactly packed grains. The grains comprised a mixture of Cu_2O and CuO nanoparticles, which will be discussed using X-ray diffraction (XRD) analysis. Noticeably, CuO nanowires were rarely observed on the surface of the urea-treated Cu−Cu_2O−CuO photoelectrode. It is known that the growth of the CuO nanowire is induced by the inward diffusion of excess oxygen from the air during heat treatment to oxidize the underneath Cu_2O layer and Cu foil. The lack of oxygen during the urea treatment is, therefore, suppressing the formation of CuO nanowires. The SEM image of the thin film before the subsequent calcination (Figure S1) shows that the surface was covered by a compact layer of particles or grains, and no CuO nanowire was observed. This indicates that urea treatment could suppress the formation of CuO, which is consistent with a previous report.[23] Cu_3N was formed during urea treatment (Figure S2). It is notable that Cu_3N was detected while CuO was not yet formed. Evidence can be found by peaks located at 23.3°, 41.0°, and 47.7°, corresponding to a cubic crystalline Cu_3N (JCPDS Card No. 04-004-2215). Cu_3N was later confirmed as being an intermediate because it

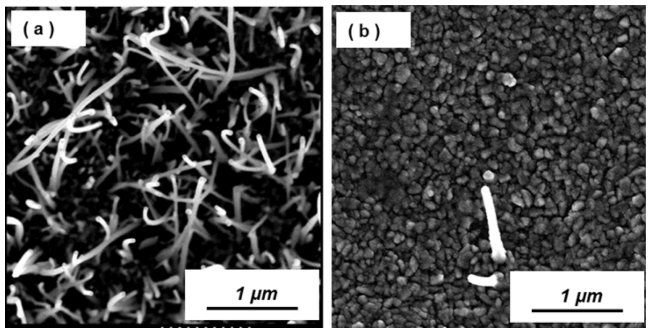

Figure 1. Top-view SEM images of Cu−Cu_2O−CuO composite photoelectrodes obtained through (a) air calcination and (b) urea treatment. An air-calcined photoelectrode was prepared by calcination of the as-anodized Cu_2O thin film at 400 °C for 1 h in an air atmosphere. The urea-treated photoelectrode was prepared by calcination of the as-anodized Cu_2O thin film with 100 mg of urea at 400 °C for 3 h in a N_2 atmosphere, followed by the second calcination at 400 °C for 1 h in an air atmosphere.

DOI: 10.1021/acsami.5b06601
ACS Appl. Mater. Interfaces 2015, 7, 19887−19893

disappeared upon the subsequent calcination. The thickness of the oxide layer is estimated to be ~20 μm (Figure S3).

The XRD pattern in Figure 2a illustrates that Cu_2O was formed by the oxidation of the anodized Cu substrate in air at

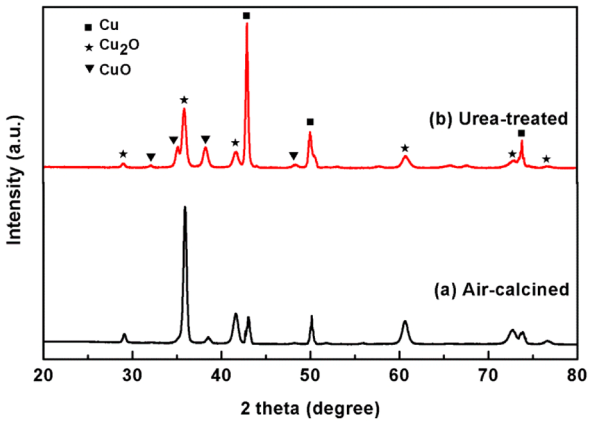

Figure 2. XRD patterns of (a) air-calcined and (b) urea-treated Cu−Cu_2O−CuO composite photoelectrodes.

400 °C for 1 h. The most intense peak located at 36.4° was assigned to the (111) plane of cubic crystalline Cu_2O (JCPDS Card No. 01-078-2076). A tiny peak at 38.7° indicated the presence of monoclinic CuO with a (111) orientation (JCPDS Card No. 01-080-1916). The peak intensity for metallic Cu (foil) was significantly smaller than that of Cu_2O, which indicates the effective oxidation of underlayer metallic copper foil by the air. With urea treatment, the intensity of the Cu_2O (111) peak at 36.4° decreased with a corresponding increase in the intensity of the CuO (111) peak at 38.7°, implying the growing amount of CuO at the expense of Cu_2O. However, as indicated from SEM top-view images (Figure 1), significantly fewer CuO nanowires were observed for the urea-treated Cu−Cu_2O−CuO photoelectrode. Upon urea treatment, instead of nanowires, the CuO component exists in the form of particles or grains on the surface. To investigate it, XPS as a surface chemical analysis technique was conducted to measure the surface concentration of CuO. Core level XPS of Cu 2p (Figure S4) shows that the surface of the urea-treated photoelectrode was solely covered by the CuO component. This is also in good agreement with previous reports that CuO was present on the surface of Cu_2O as a stable layer.[24,25] Another interesting finding is that the metallic Cu (111) peak (2θ = 43.3°) in the urea-treated thin film showed an intensity much higher than that in the air-calcined thin film. This indicates that urea treatment was able to preserve Cu in the oxide thin film from being oxidized into copper oxide during calcination. During urea treatment, the as-anodized Cu_2O thin film was annealed with urea at 400 °C for 3 h in a N_2 atmosphere, producing Cu_3N (Figure S2).[26] The diffusion of active nitrogen species generated from the decomposed urea resulted in the formation of Cu_3N within the oxidized layer. The Cu_3N (as the intermediate component) was oxidized during the final calcination step, and that minimized the further oxidation of the bulk Cu_2O and the bottom Cu substrate.[27] As a result, formation of CuO nanowires was suppressed, as well. Only the Cu_2O layer on the surface of the thin film was more likely to be oxidized into CuO particles. This is in good agreement with the SEM top-view images and XPS surface analysis. Cu_3N was not detected in the final product of the urea-treated Cu−Cu_2O−CuO photoelectrode. It is highly possible that residual nitrogen could remain in the thin film as the duration for subsequent air calcination was brief, which is further proved by XPS N 1s (Figure 3b). Because metallic Cu is more conductive than

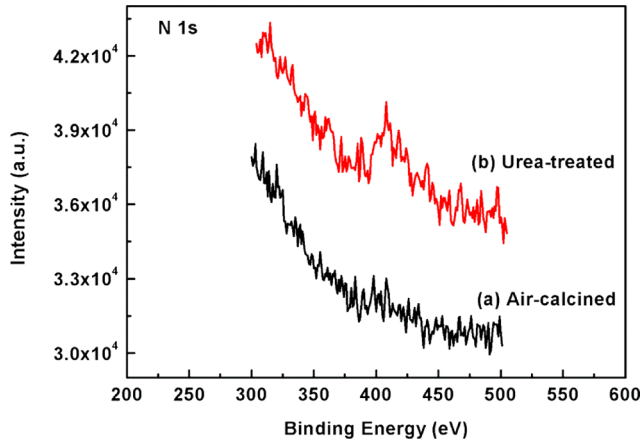

Figure 3. XPS N 1s of (a) air-calcined and (b) urea-treated Cu−Cu_2O−CuO composite photoelectrodes.

Cu_2O and CuO, the preservation of metallic Cu in the urea-treated Cu−Cu_2O−CuO composite photoelectrode significantly reduced its charge transfer resistance, which will be confirmed by Mott−Schottky measurements and electrochemical impedance spectroscopy in the following discussion.

XPS spectra in Figure 3 confirmed the existence of residual nitrogen at a low concentration in the urea-treated Cu−Cu_2O−CuO composite photoelectrode. As shown in Figure 3a, no N-related peaks were measured for the air-calcined Cu−Cu_2O−CuO photoeletrode. The peak with a binding energy of 408.0 eV confirmed the presence of nitrogen in the urea-treated Cu−Cu_2O−CuO photoelectrodes, in the form of the nitrate state.[26] As described, Cu_3N was present as the intermediate component after calcination with urea at 400 °C for 3 h in a N_2 atmosphere (Figure S2). During the second calcination in air, Cu_3N was transformed into copper oxide, as proven by the increased amount of CuO at the expense of Cu_3N. The nitrogen species observed in XPS might have resulted from the remaining trace Cu_3N (beyond the detection limit of XRD), or it could be possibly due to the doping of nitrogen into the crystal structure of the Cu_2O−CuO thin film. The distortion or changes in crystal structure of CuO or Cu_2O induced by this minimal amount of dopant are usually unnoticeable from the bulk XRD analysis. However, it has been widely accepted that the impurities (such as nitrogen) in semiconductors played an imperative role in their electrical and optical properties.

The conduction type and carrier concentration of the air-calcined and urea-treated Cu−Cu_2O−CuO composite photoelectrodes were determined using Mott−Schottky measurements at a frequency of 10 kHz. As shown in Figure 4a, the MS plots of both photoelectrodes showed a negative slope, verifying their p-type semiconducting behavior. Equation 1 shows that the charge carrier density of the electrode is inversely proportional to the slope of the MS plots. It is obvious that the charge carrier density of the urea-treated Cu−Cu_2O−CuO electrode was significantly improved.

$$N_a = (2/e_0\varepsilon\varepsilon_0)[d(1/C^2)/dV]^{-1} \quad (1)$$

DOI: 10.1021/acsami.5b06601
ACS Appl. Mater. Interfaces 2015, 7, 19887−19893

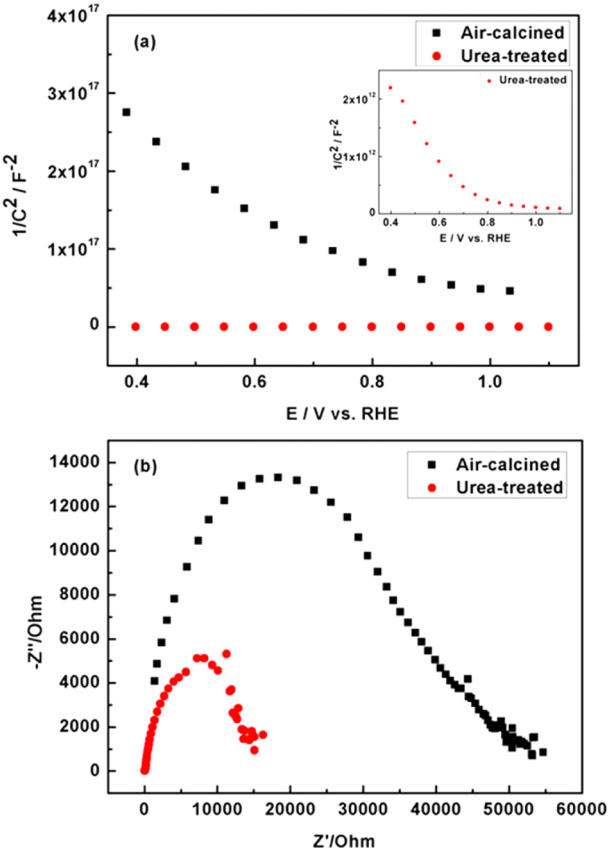

Figure 4. (a) Mott–Schottky and (b) Nyquist plots of air-calcined and urea-treated Cu–Cu_2O–CuO composite photoelectrodes.

where N_a is the carrier density of the photoelectrode, e_0 is the electron charge, ε is the dielectric constant, ε_0 is the permittivity of a vacuum, C is the interfacial capacitance, and V is the applied bias at the electrode.[27]

As the MS estimation is built on the basis of a flat electrode model, the current air-calcined and urea-treated photoelectrodes do not perfectly fit in. The exact value of carrier density may not be accurate. Furthermore, the coexistence of Cu, Cu_2O, and CuO imposes a great challenge in producing the accurate value for an individual component. However, qualitative comparison of the overall charge carrier density of the photoelectrodes between air-calcined and urea-treated Cu–Cu_2O–CuO is appropriate. It is estimated that the carrier density of the urea-treated photoelectrode was 5 orders of magnitude higher than that of the air-calcined sample. The similar thickness of the oxidized layer of copper (Cu_2O and CuO) in the air-calcined and urea-treated photoelectrodes (Figure S3) eliminated the possibility that a higher carrier density could be attributed to a larger amount of oxides in the urea-treated photoelectrode. On the basis of our results, it is believed that the urea treatment improved the carrier density of the Cu–Cu_2O–CuO photoelectrode through the preservation of metallic Cu, in which it happened via the formation of the Cu_3N intermediate. The presence of a larger amount of metallic Cu also increased the bulk conductance of the Cu–Cu_2O–CuO photoelectrode. In addition, copper vacancies might be generated during the conversion of Cu_3N to oxide of copper upon calcination. Constructive effects of the Cu vacancy in generating a higher carrier density have been reported previously.[28,29] Besides, other works from the literature suggested the trace doping of nitrogen into the photoelectrodes may increase the carrier density of Cu_2O.[14,30,31] On the basis of the Mott–Schottky data, the flat band potential can be determined by the extrapolation of the MS plot. The flat band potentials of air-calcined and urea-treated thin films (Figure S5) were positioned at 0.72 and 0.73 V versus RHE, respectively. These values are comparable to the reported flat band potentials in the literature reports.[32]

The charge transfer kinetics of the air-calcined and urea-treated Cu–Cu_2O–CuO composite photoelectrodes was measured by electrochemical impedance spectroscopy. Figure 4b shows the Nyquist plots of the air-calcined and urea-treated Cu–Cu_2O–CuO composite photoelectrodes. The radius of the semicircle is correlated to the charger transfer resistance at the interface and charge transfer ability of the photoelectrode. The urea-treated photoelectrode exhibited a much smaller semicircle radius of the Nyquist plot, which indicated a lower charge transfer resistance because of the more efficient electron-conducting pathway.[33,34] The decrease in charger transfer resistance in the urea-treated photoelectrode is attributed to the preservation of metallic Cu, which is more conductive than copper oxide and facilitates electron transfer. Another possible reason is the enhancement of carrier density resulted from preservation of Cu and possible doping of nitrogen. This is also supported by other research that showed that nitrogen was reported as an effective dopant in reducing the resistivity of a Cu_2O film.[12,13]

To investigate the effect of urea treatment on the charge transfer behavior, the time-resolved fluorescence lifetimes of the commercial Cu_2O (as reference) and air-calcined and urea-treated Cu–Cu_2O–CuO composite photoelectrodes were compared and measured at 405 nm using TCSPC, as shown in Figure 5. The electron transfer time was calculated by fitting

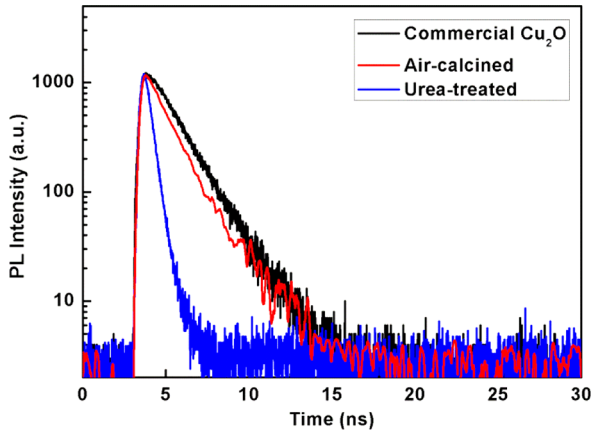

Figure 5. Transient decay curves of commercial Cu_2O and air-calcined and urea-treated Cu–Cu_2O–CuO composite photoelectrodes at 405 nm.

a biexponential function to the fluorescence decay using listed eqs 2 and 3.

$$y = A_1 \exp(-t/\tau_1) + A_2 \exp(-t/\tau_2) \quad (2)$$

$$\langle\tau\rangle = (A_1\tau_1 + A_2\tau_2)/(A_1A_2) \quad (3)$$

where τ_1 and τ_2 are the fluorescence lifetime of the fast decay component and slow decay component, respectively, and A_1 and A_2 are the corresponding amplitudes.

DOI: 10.1021/acsami.5b06601
ACS Appl. Mater. Interfaces 2015, 7, 19887–19893

The reference Cu_2O foil was prepared by spin coating the commercial Cu_2O powder onto Cu substrate, and the electron transfer time for the commercial Cu_2O was estimated to be 1.63 ± 0.2 ns. Because of the assistance of CuO in promoting the photogenerated electron transfer from Cu_2O to CuO, the air-calcined Cu−Cu_2O−CuO photoelectrode exhibited a slightly shorter electron transfer time of 1.40 ± 0.2 ns. The shortest electron transfer time of 0.38 ± 0.2 ns was observed for the urea-treated Cu−Cu_2O−CuO composite photoelectrode. First, a relatively larger amount of CuO nanoparticles within the Cu_2O-dominant urea-treated photoelectrode is more efficient in accelerating photogenerated electron transfer from Cu_2O to CuO. Second, the presence of nitrogen in the urea-treated photoelectrode might also play a role in separating and transferring photogenerated electrons and holes. Third, the preserved metallic Cu in the urea-treated photoelectrode might form a Schottky barrier of Cu−Cu_2O at the interface, where Cu nanoparticles as electron sinks are favorable for the separation of photogenerated electron−hole pairs and electron transfer.[35] The acceleration of photogenerated electron transfer in the urea-treated photoelectrodes could minimize the recombination of electrons and holes, thus minimizing the photocurrent decay during photoelectrochemical measurement.

To investigate the photoelectrochemical responses and stability of the air-calcined and urea-treated Cu−Cu_2O−CuO composite photoelectrodes, the photocurrent and their corresponding current decay rate were measured in a standard three-electrode photoelectrochemical system. As shown in Figure 6, upon visible light illumination (>420 nm), electrons and holes were generated in the Cu−Cu_2O−CuO composite photoelectrode. Because of its p-type characteristic, electrons were driven from the Pt counter electrode to the Cu−Cu_2O−CuO composite working photoelectrode to generate a cathodic photocurrent (Figure 7). This observation of the conduction type is consistent with the Mott−Schottky analyses. The urea-treated photoelectrode exhibited an initial photocurrent of 2.20 mA/cm^2, which was almost double the value of the air-calcined sample (1.20 mA/cm^2). The higher carrier density and the lower charge transfer resistance accounted for the enhanced photocurrent. Figure 7 illustrates the schematic energy diagram of the Cu−Cu_2O−CuO photoelectrode. The preservation of underlayer Cu as an electron conductor upon urea treatment provides a more efficient pathway for electron transfer from the Pt counter electrode to the Cu_2O−CuO composite. The typical air-calcined anodized Cu thin film usually contains less metallic Cu underneath (as indicated in the XRD data) as the oxidation is fast and rather uncontrolled. As the conduction band of Cu_2O is located at a state higher in energy than that of CuO, this suitable band energy alignment also promotes the electron transfer from Cu_2O to CuO at the junction. With the downward band bending at the electrolyte interface facilitated by the voltage, the higher charge carrier density induced by the presence of nitrogen (possibly as the dopant), and the higher film conductance, the charge population that could be effectively responsible for photocurrent generation is therefore larger. Note that the visible light absorption for both air-calcined and urea-treated Cu−Cu_2O−CuO thin films is comparable and, therefore, unlikely to contribute to the differences observed in this experiment (Figure S6).

With the on−off illumination cycles, both photoelectrodes suffered photocurrent decay most possibly because of the photocorrosion of Cu_2O. As both the reduction and oxidation potentials of Cu_2O lie in the bandgap of Cu_2O, the photocorrosion of Cu_2O was considered as the main competitive reaction to hydrogen generation.[36] The photocurrent decay curves were plotted on the diminished photocurrent against its initial value. After 10 on−off illumination cycles for 40 min, the urea-treated photoelectrode managed to maintain 50% of its initial photocurrent, which was 20% higher than that of the air-calcined photoelectrode. A combination of several factors was taken into consideration. As we reported before, the air-calcined photoelectrode embedded

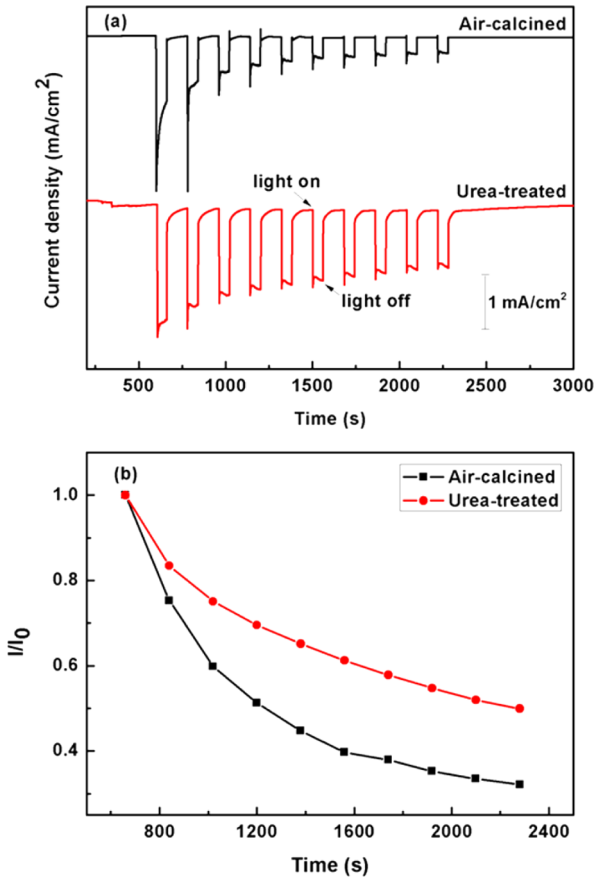

Figure 6. (a) Photoelectrochemical responses and (b) corresponding current decay of air-calcined and urea-treated Cu−Cu_2O−CuO composite photoelectrodes.

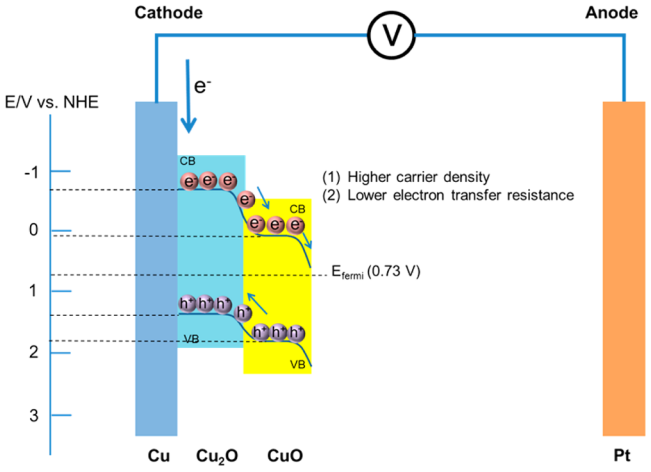

Figure 7. Schematic energy diagram of the Cu−Cu_2O−CuO photoelectrode.

DOI: 10.1021/acsami.5b06601
ACS Appl. Mater. Interfaces 2015, 7, 19887−19893

with CuO nanowires was beneficial for improving the mechanical stability of Cu_2O as it improved the adhesion of the oxide layer to the Cu substrate.[21] These CuO nanowires that covered the surface of Cu_2O (Figure 1a) were helpful in transporting electrons photogenerated from Cu_2O and lowering the redox activity at the surface of Cu_2O. When the Cu−Cu_2O−CuO photoelectrode was treated with urea, instead of nanowires, a compact outer layer of CuO nanoparticles was formed on the electrode surface, as proven by SEM, XRD, and XPS. A layer of compact surface CuO is more effective in covering the whole surface of Cu_2O to minimize the surface redox reaction of Cu_2O with the aqueous solution. In addition, because of the well-matched band energy alignment of Cu_2O and CuO, the transfer of photogenerated electrons in Cu_2O to CuO is thermodynamically favored.[37] The compact layer of CuO in the urea-treated photoelectrode provides more efficient electron transfer between Cu_2O and CuO and slows the gradual photocorrosion of Cu_2O more effectively. The photocurrent decay is also associated with the recombination rate of photogenerated electron−hole pairs. The TCSPC results demonstrate that the preservation of Cu and the presence of nitrogen in the urea-treated photoelectrode were beneficial in accelerating the electron transfer, leaving less significant recombination to contribute to the current decay.

4. CONCLUSIONS

To conclude, metallic Cu was preserved and nitrogen was incorporated into the Cu−Cu_2O−CuO composite photoelectrode synthesized by anodization of Cu foil followed by thermal treatment with urea. The charge carrier density of the urea-treated photoelectrode was approximately 5 orders of magnitude higher than that of the air-calcined photoelectrode, accompanied by the lower charge transfer resistance measured using electrochemical impedance spectroscopy. A much faster electron transfer time of 0.38 ns was measured on the urea-treated Cu−Cu_2O−CuO composite photoelectrode using the time-correlated single-photon counting method in comparison with 1.40 ns for conventionally air-treated Cu−Cu_2O−CuO and 1.63 ns for commercial Cu_2O. The preservation of metallic Cu and the presence of nitrogen in the urea-treated photoelectrode played a crucial role in the enhancement of carrier density, the decrease in charge transfer resistance, and the acceleration of electron transfer. Urea treatment also resulted in the formation of a layer of compact CuO on the surface that is more effective in preventing the photocorrosion of Cu_2O. All changes in these properties made the urea-treated Cu−Cu_2O−CuO composite photoelectrode highly photocatalytic and more stable in a photoelectrochemical system.

■ ASSOCIATED CONTENT

Supporting Information

The Supporting Information is available free of charge on the ACS Publications website at DOI: 10.1021/acsami.5b06601.

SEM image of the as-anodized Cu_2O thin film after calcination with 100 mg of urea at 400 °C for 3 h in a N_2 atmosphere, cross-section SEM images of air-calcined and urea-treated thin films, XRD patterns of the intermediate Cu_3N, core level XPS of Cu 2p of urea-treated Cu−Cu_2O−CuO composite photoelectrodes, Mott−Schottky plots of air-calcined and urea-treated Cu−Cu_2O−CuO composite photoelectrodes, and UV−vis spectra of air-calcined and urea-treated Cu−Cu_2O−CuO composite photoelectrodes (PDF)

■ AUTHOR INFORMATION

Corresponding Authors

*E-mail: yh.ng@unsw.edu.au.
*E-mail: r.amal@unsw.edu.au.

Author Contributions

P.W. designed and conducted the experiments, synthesized the photoelectrodes, conducted characterizations, and wrote the manuscript. Y.T. helped with UV−vis measurement and discussion. X.W. took the TCSPC measurements and conducted the analysis. R.A. and Y.H.N. supervised this project and helped interpret the results. All authors were involved in analysis of data and completion of this paper.

Notes

The authors declare no competing financial interest.

■ ACKNOWLEDGMENTS

This work was financially supported by the Australia Research Council Discovery Project (DP 110101638). P.W. acknowledges the financial support from the China Scholarship Council. We also acknowledge the UNSW Mark Wainwright Analytical Centre for providing facilities and training, especially Dr. Bill Gong from Solid State & Elemental Analysis for his help in XPS measurement.

■ REFERENCES

(1) Sui, Y.; Zeng, Y.; Zheng, W.; Liu, B.; Zou, B.; Yang, H. Synthesis of Polyhedron Pollow Structure Cu2O and Their Gas-sensing Properties. *Sens. Actuators, B* **2012**, *171−172* (0), 135−140.

(2) Wei, S.; Shi, J.; Ren, H.; Li, J.; Shao, Z. Fabrication of Ag/Cu2O Composite Films with a Facile Method and Their Photocatalytic Activity. *J. Mol. Catal. A: Chem.* **2013**, *378* (0), 109−114.

(3) Chen, L.-C. Review of Preparation and Optoelectronic Characteristics of Cu2O-based Solar Cells with Nanostructure. *Mater. Sci. Semicond. Process.* **2013**, *16* (5), 1172−1185.

(4) Morales-Guio, C. G.; Tilley, S. D.; Vrubel, H.; Grätzel, M.; Hu, X. Hydrogen Evolution from a Copper(I) Oxide Photocathode Coated with an Amorphous Molybdenum Sulphide Catalyst. *Nat. Commun.* **2014**, *5*, 3059.

(5) Pollack, G. P.; Trivich, D. Photoelectric Properties of Cuprous Oxide. *J. Appl. Phys.* **1975**, *46* (1), 163−172.

(6) Li, Y.; Zhang, J. Hydrogen Generation from Photoelectrochemical Water Splitting Based on Nanomaterials. *Laser Photonics Rev.* **2010**, *4* (4), 517−528.

(7) Shockley, W.; Queisser, H. J. Detailed Balance Limit of Efficiency of p-n Junction Solar Cells. *J. Appl. Phys.* **1961**, *32* (3), 510−519.

(8) Wang, L.; Tao, M. Fabrication and Characterization of p-n Homojunctions in Cuprous Oxide by Electrochemical Deposition. *Electrochem. Solid-State Lett.* **2007**, *10* (9), H248−H250.

(9) Garuthara, R.; Siripala, W. Photoluminescence Characterization of Polycrystalline n-type Cu2O Films. *J. Lumin.* **2006**, *121* (1), 173−178.

(10) Han, X.; Han, K.; Tao, M. Characterization of Cl-doped n-type Cu2O Prepared by Electrodeposition. *Thin Solid Films* **2010**, *518* (19), 5363−5367.

(11) Scanlon, D. O.; Watson, G. W. Undoped n-Type Cu2O: Fact or Fiction? *J. Phys. Chem. Lett.* **2010**, *1* (17), 2582−2585.

(12) Lai, G.; Wu, Y.; Lin, L.; Qu, Y.; Lai, F. Low Resistivity of N-doped Cu2O Thin Films Deposited by Rf-magnetron Sputtering. *Appl. Surf. Sci.* **2013**, *285* (Part B), 755−758.

(13) Malerba, C.; Azanza Ricardo, C. L.; D'Incau, M.; Biccari, F.; Scardi, P.; Mittiga, A. Nitrogen Doped Cu2O: A Possible Material for

DOI: 10.1021/acsami.5b06601
ACS Appl. Mater. Interfaces 2015, 7, 19887−19893

Intermediate Band Solar Cells? *Sol. Energy Mater. Sol. Cells* **2012**, *105*, 192−195.
(14) Ishizuka, S.; Kato, S.; Maruyama, T.; Akimoto, K. Nitrogen Doping into Cu2O Thin Films Deposited by Reactive Radio-frequency Magnetron Sputtering. *Jpn. J. Appl. Phys.* **2001**, *40* (4B), 2765−2768.
(15) Zhao, Z.; He, X.; Yi, J.; Ma, C.; Cao, Y.; Qiu, J. First-principles Study on the Doping Effects of Nitrogen on the Electronic Structure and Optical Properties of Cu2O. *RSC Adv.* **2013**, *3* (1), 84−90.
(16) Li, H. J.; Pu, C. Y.; Ma, C. Y.; Li, S.; Dong, W. J.; Bao, S. Y.; Zhang, Q. Y. Growth Behavior and Optical Properties of N-doped Cu2O Films. *Thin Solid Films* **2011**, *520*, 212−216.
(17) Nakano, Y.; Saeki, S.; Morikawa, T. Optical Bandgap Widening of p-type Cu2O Films by Nitrogen Doping. *Appl. Phys. Lett.* **2009**, *94* (2), 022111.
(18) Zhang, L.; McMillon, L.; McNatt, J. Gas-dependent Bandgap and Electrical Conductivity of Cu2O Thin Films. *Sol. Energy Mater. Sol. Cells* **2013**, *108* (0), 230−234.
(19) Cheng Siah, S.; Seog Lee, Y.; Segal, Y.; Buonassisi, T. Low Contact Resistivity of Metals on Nitrogen-doped Cuprous Oxide (Cu2O) Thin-films. *J. Appl. Phys.* **2012**, *112* (8), 084508.
(20) Asahi, R.; Morikawa, T.; Ohwaki, T.; Aoki, K.; Taga, Y. Visible-Light Photocatalysis in Nitrogen-Doped Titanium Oxides. *Science* **2001**, *293* (5528), 269−271.
(21) Wang, P.; Ng, Y. H.; Amal, R. Embedment of Anodized p-type Cu2O Thin Films with CuO Nanowires for Improvement in Photoelectrochemical Stability. *Nanoscale* **2013**, *5* (7), 2952−2958.
(22) Wang, P.; Wen, X.; Amal, R.; Ng, Y. H. Introducing a Protective Interlayer of TiO2 in Cu2O-CuO Heterojunction Thin Film as a Highly Stable Visible Light Photocathode. *RSC Adv.* **2015**, *5* (7), 5231−5236.
(23) Li, H. J.; Pu, C. Y.; Ma, C. Y.; Li, S.; Dong, W. J.; Bao, S. Y.; Zhang, Q. Y. Growth Behavior and Optical Properties of N-doped Cu2O Films. *Thin Solid Films* **2011**, *520* (1), 212−216.
(24) Nayeb Sadeghi, S.; Shafiekhani, A.; Vesaghi, M. A. Direct Production of Carbon Nanotubes Decorated with Cu2O by Thermal Chemical Vapor Deposition on Ni Catalyst Electroplated on a Copper Substrate. *J. Nanopart. Res.* **2011**, *13* (10), 4681−4689.
(25) Martis, P.; Fonseca, A.; Mekhalif, Z.; Delhalle, J. Optimization of Cuprous Oxide Nanocrystals Deposition on Multiwalled Carbon Nanotubes. *J. Nanopart. Res.* **2010**, *12* (2), 439−448.
(26) Bacsa, R.; Kiwi, J.; Ohno, T.; Albers, P.; Nadtochenko, V. Preparation, Testing and Characterization of Doped TiO2 Active in the Peroxidation of Biomolecules under Visible Light. *J. Phys. Chem. B* **2005**, *109* (12), 5994−6003.
(27) Wang, G.; Ling, Y.; Wang, H.; Yang, X.; Wang, C.; Zhang, J. Z.; Li, Y. Hydrogen-treated WO3 Nanoflakes Show Enhanced Photostability. *Energy Environ. Sci.* **2012**, *5* (3), 6180−6187.
(28) Hsu, S.-W.; Bryks, W.; Tao, A. R. Effects of Carrier Density and Shape on the Localized Surface Plasmon Resonances of Cu2−xS Nanodisks. *Chem. Mater.* **2012**, *24* (19), 3765−3771.
(29) Ma, J.; Wei, S.-H.; Gessert, T. A.; Chin, K. K. Carrier Density and Compensation in Semiconductors with Multiple Dopants and Multiple Transition Energy Levels: Case of Cu Impurities in CdTe. *Phys. Rev. B: Condens. Matter Mater. Phys.* **2011**, *83* (24), 245207.
(30) Ishizuka, S.; Maruyama, T.; Akimoto, K. Thin-film Deposition of Cu2O by Reactive Radio-frequency Magnetron Sputtering. *Jpn. J. Appl. Phys.* **2000**, *39* (Part 2, No. 8A), L786−L788.
(31) Lu, Y.-M.; Chen, C.-Y.; Lin, M. H. Effect of Hydrogen Plasma Treatment on the Electrical Properties of Sputtered N-doped Cuprous Oxide Films. *Mater. Sci. Eng., B* **2005**, *118* (1−3), 179−182.
(32) Li, C.; Li, Y.; Delaunay, J.-J. A Novel Method to Synthesize Highly Photoactive Cu2O Microcrystalline Films for Use in Photoelectrochemical Cells. *ACS Appl. Mater. Interfaces* **2014**, *6* (1), 480−486.
(33) Hou, Y.; Li, X. Y.; Zhao, Q. D.; Quan, X.; Chen, G. H. Fabrication of Cu2O/TiO2 Nanotube Heterojunction Arrays and Investigation of its Photoelectrochemical Behavior. *Appl. Phys. Lett.* **2009**, *95* (9), 093108.
(34) Bell, N. J.; Ng, Y. H.; Du, A.; Coster, H.; Smith, S. C.; Amal, R. Understanding the Enhancement in Photoelectrochemical Properties of Photocatalytically Prepared TiO2-Reduced Graphene Oxide Composite. *J. Phys. Chem. C* **2011**, *115* (13), 6004−6009.
(35) Sun, S.; Kong, C.; You, H.; Song, X.; Ding, B.; Yang, Z. Facet-selective Growth of Cu-Cu2O Heterogeneous Architectures. *CrystEngComm* **2012**, *14* (1), 40−43.
(36) Paracchino, A.; Laporte, V.; Sivula, K.; Grätzel, M.; Thimsen, E. Highly Active Oxide Photocathode for Photoelectrochemical Water Reduction. *Nat. Mater.* **2011**, *10* (6), 456−461.
(37) Ng, C.; Iwase, A.; Ng, Y. H.; Amal, R. Transforming Anodized WO3 Films into Visible-Light-Active Bi2WO6 Photoelectrodes by Hydrothermal Treatment. *J. Phys. Chem. Lett.* **2012**, *3* (7), 913−918.

DOI: 10.1021/acsami.5b06601
ACS Appl. Mater. Interfaces 2015, 7, 19887−19893